Citation: Oncogenesis (2012) **1**, e13; doi:10.1038/oncsis.2012.13

www.nature.com/oncsis

ORIGINAL ARTICLE

The RhoGAP protein Deleted in Liver Cancer 3 (DLC3) is essential for adherens junctions integrity

G Holeiter[1,3], A Bischoff[1,3], AC Braun[1], B Huck[1], P Erlmann[1,4], S Schmid[1], R Herr[2], T Brummer[2] and MA Olayioye[1]

Epithelial cell–cell contacts are mediated by E-cadherin interactions, which are regulated by the balanced local activity of Rho GTPases. Despite the known function of Rho at adherens junctions (AJs), little is known about the spatial control of Rho activity at these sites. Here we provide evidence that in breast epithelial cells the Deleted in Liver Cancer 3 (DLC3) protein localizes to AJs and is essential for E-cadherin function. DLC3 is a still poorly characterized RhoA-specific GTPase-activating protein that is frequently downregulated in various types of cancer. We demonstrate that DLC3 depletion leads to mislocalization of E-cadherin and catenins, which was associated with impaired cell aggregation and increased migration. This is explained by aberrant local Rho signaling because ROCK inhibition restored cell–cell contacts in DLC3 knockdown cells. We thus identify DLC3 as a novel negative regulator of junctional Rho and propose that DLC3 loss contributes to carcinogenesis by compromising epithelial integrity.

Oncogenesis (2012) **1,** e13; doi:10.1038/oncsis.2012.13; published online 4 June 2012

Subject Categories: molecular oncology

Keywords: Deleted in Liver Cancer 3/StarD8; E-cadherin; tumor suppressor; cell polarization and motility

INTRODUCTION

Epithelial tissues are characterized by their polarized morphology, specialized cell–cell contacts and attachment to an underlying basement membrane. Adherens junctions (AJs) are sites of epithelial cell–cell contact that are primarily maintained by E-cadherin, a membrane-spanning protein whose extracellular domains engage in calcium-dependent homotypic interactions between E-cadherin molecules on adjacent cells. The cytoplasmic parts directly interact with β-catenin and p120-catenin that bridge the complex with the actin cytoskeleton. This highly organized molecular network required for an intact epithelial architecture is commonly disrupted during the development of epithelial cancers.[1,2]

Cell adhesion is a dynamic process in which the cadherin–catenin complex and the attached cytoskeleton undergo constant remodeling. Rho GTPases (RhoA, Rac and Cdc42) have been shown to participate in these processes, as they are necessary for the formation and maintenance of cadherin-mediated cell–cell contacts, as well as for cytoskeletal reorganization and apico-basolateral polarization.[3,4] Spatiotemporal analysis with FRET biosensors revealed that RhoA is active during *de novo* cell adhesion, but activity is restricted to the periphery of contacting cell membranes.[5] At later stages, RhoA is required for the formation of actomyosin filaments, which in turn stabilize cell adhesion and participate in the development of the polarized epithelial phenotype.[3,4] Rho can regulate AJs in two opposing ways through the effectors Rho-associated protein kinase (ROCK) and Dia1.[6] ROCK is a serine-threonine kinase that phosphorylates and inactivates myosin light chain (MLC) phosphatase, thereby stabilizing phosphorylated active MLC and generating contractile forces that lead to AJ disruption. In addition, ROCK can phosphorylate MLC directly.[7] The formin Dia1 is important for actin polymerization and ensures the maintenance and stabilization of AJs.[6,8] The downstream pathway engaged appears to depend on the level of active Rho, as low levels favor signaling through Dia1, whereas higher levels are required for efficient ROCK activation.[6] The precise pathway mediating cell–cell adhesion may also depend on the cell type, because in mouse keratinocytes and human bronchial epithelial cells the Rho effector protein PRK2 was found to be required for the maturation of apical junctions[9,10]

Rho activity is controlled by GEFs (guanine nucleotide exchange factors), which promote the exchange of GDP for GTP thereby activating Rho proteins, and GAPs (GTPase-activating proteins), which accelerate the intrinsic rate at which Rho hydrolyzes bound GTP to GDP and hence becomes inactivated.[11] Little is known about the molecular mechanisms that ensure spatially restricted Rho activation at AJs. Recently, p114RhoGEF was identified as the first GEF protein responsible for RhoA activation during epithelial junction formation and maturation,[12] whereas GEF-H1 was previously reported to be required for RhoA activation during adhesion disassembly.[13] Thus far, the GAP protein described to be involved in the regulation of junctional RhoA is p190RhoGAP during conditions of Rac activation.[14] By stabilizing the phosphorylated, active form of p190RhoGAP, Rac antagonizes Rho signaling in many cell types.[15,16] In the context of cell–cell adhesion, Rac activation in fibroblasts was shown to trigger p190RhoGAP membrane translocation to regulate AJs via RhoA inactivation.[14]

Three genes of the human genome, DLC1, DLC2 and DLC3 (Deleted in Liver Cancer 3), encode for the DLC subfamily of

[1]Institute of Cell Biology and Immunology, University of Stuttgart, Stuttgart, Germany and [2]Center for Biological Systems Analysis, Faculty for Biology and Centre for Biological Signalling Studies BIOSS, Albert-Ludwigs University Freiburg, Freiburg, Germany. Correspondence: Professor Dr MA Olayioye, Institute of Cell Biology and Immunology, University of Stuttgart, Allmandring 31, Baden-Württemberg, Stuttgart 70569, Germany.
E-mail: monilola.olayioye@izi.uni-stuttgart.de
[3]These authors contributed equally to this work.
[4]Current address: Centre de Regulació Genòmica, Cell and Developmental Biology, Dr Aiguader 88, Barcelona 08003, Spain
Received 11 April 2012; accepted 26 April 2012

RhoGAP proteins.[17] DLC proteins are composed of an aminoterminal sterile α motif (SAM), a RhoA-specific GAP domain and a carboxyterminal steroidogenic acute regulatory protein-related lipid transfer (START) domain. SAM domains mediate protein interactions, whereas START domains are lipid-binding modules, whose function in the DLC proteins has not been characterized. The best studied family member DLC1 is frequently deleted in various types of human cancers and a tumor suppressive function has been established *in vivo*. In a mouse model of hepatocellular carcinoma, DLC1 loss cooperated with c-myc expression in tumor development[18] and re-expression of DLC1 in highly invasive breast cancer cells reduced the frequency of lung metastasis.[19] Although there are reports on GAP-independent functions of DLC1, its tumor suppressive function appears to be primarily mediated by the GAP activity, and is thought to require the interaction with tensin adapter proteins that recruit the protein to focal adhesions.[20–22] By contrast, the DLC3 protein is still poorly characterized. Here we define for the first time a physiological function for DLC3 in the spatial regulation of Rho signaling at AJs that ensures the maintenance of E-cadherin-based cell–cell contacts.

RESULTS

Ectopically expressed DLC3 localizes to sites of cell–cell contact and impairs breast epithelial cell differentiation

Rho GTPases are active at various subcellular sites where they are locally regulated by specific GEFs and GAPs. Analysis of the localization of these regulators may thus provide insight into the nature of the Rho-dependent processes they control. The DLC3 gene located on chromosome Xq13 gives rise to two alternative transcripts, DLC3α and DLC3β, which lacks the aminoterminal SAM.[23] The cellular function of DLC3α/β is largely unknown, partly due to the lack of commercially available antibodies that detect the endogenous protein. Because even low-level transient expression of DLC3 induced severe morphological changes, we generated MCF7 breast carcinoma sublines stably expressing GFP-tagged DLC3 to first analyze its subcellular localization. Interestingly, in confluent cell monolayers GFP–DLC3α was found to co-localize with E-cadherin at sites of cell–cell contact (Figure 1a). This was independent of the DLC3 GAP activity because an inactivating mutation within the GAP domain (K725E) did not alter the localization (Figure 1a). GFP–DLC3β also localized to cell–cell contacts, indicating that the SAM domain is not required for targeting to these sites (Supplementary Figure S1). The GAP activity and specificity of the DLC3 variants was verified using previously described Rho biosensors[24] (Supplementary Figure S2). Compared with the controls, DLC3α and DLC3β strongly reduced the emission ratio (FRET/CFP) of the RhoA biosensor, whereas DLC3α–K725E and DLC3β–K645E only had minimal effects. DLC3α was reported to also possess modest GAP activity toward Cdc42 *in vitro*,[25] but we could not detect any GAP activity using the Cdc42 and Rac1 biosensors in our system (Supplementary Figure S2).

Localization of GFP–DLC3α to cell junctions was further observed in the non-transformed human breast epithelial cell line MCF10A (Figure 1b). In 3D matrigel cultures, MCF10A cells differentiate to form acini with a polarized outer layer of cells surrounding a hollow lumen. Development of apicobasal polarity and the establishment of cell adhesion are critical for acinar morphogenesis.[26] To investigate the localization and function of DLC3 in 3D cultures, MCF10A sublines were grown in matrigel and analyzed after 6 days when polarization of acini should have occurred. In line with our previous observations, expression of GFP alone had no effect on acini differentiation,[27] whereas cells expressing the wild-type GFP–DLC3α protein grew to form multicellular structures, but failed to give rise to ordered acini (Figure 1c). Of note, cells often appeared to detach from the parental spheroid (Figure 1c). This was dependent on the GAP activity, because MCF10A cells stably expressing DLC3α–K725E developed normally (Figure 1c). DLC3α–K725E was enriched at lateral membranes and concentrated basolaterally especially at the edges of cell–cell contacts (Figure 1c). These data indicate that ectopic DLC3 expression interferes with breast epithelial cell polarization in 3D cultures.

DLC3 downregulation impairs recruitment of E-cadherin–catenin complexes to cell–cell contacts

To investigate the potential function of DLC3 on junction formation, we downregulated DLC3 in MCF7 cells using two specific siRNAs that target both α- and β-isoforms. Co-transfection of the siRNAs with a GFP-tagged DLC3α expression construct in HEK293T cells (Figure 2a) and analysis of DLC3 transcript levels upon knockdown in MCF7 cells by semi-quantitative RT–PCR (Figure 2b) revealed efficient silencing. MCF7 cells were then transfected with the DLC3-specific siRNAs and an siRNA-targeting β-galactosidase (siLacZ) as a control and stained for E-cadherin 3 days post transfection. DLC3-depleted cells demonstrated poorly defined AJs as judged by E-cadherin staining (Figure 2c). This was not due to E-cadherin downregulation because protein levels remained unchanged as determined by immunoblotting of whole cell lysates (data not shown). Moreover, recruitment of β-catenin and p120-catenin to sites of cell adhesion was severely disturbed (Figure 2c). This effect was even more pronounced when cells were replated 2 days post transfection and stained after 24 h, giving cells less time to establish mature AJs (data not shown).

DLC3 is required for adherens junction stability

We next examined the functionality of AJs by performing calcium switch experiments, in which confluent cell monolayers are treated with EGTA to disrupt calcium-dependent E-cadherin-based cell–cell contacts. To this end, control and DLC3-depleted cells were replated at high density and subjected to EGTA treatment the next day. Compared with control cells, DLC3 knockdown cells were more sensitive to calcium depletion as seen by greater retraction of cells (Figure 3a, 0 min), resulting in the delayed re-establishment of confluent cell monolayers upon EGTA washout (Figure 3a). To quantify these effects, we performed online impedance measurements of cells grown on microtiter plates arrayed with electrodes (E-plates) to determine cell contraction in response to calcium depletion. Impedance (cell index) is maximal when plates are covered with a confluent cell monolayer. Indeed, compared with the siLacZ control, cells lacking DLC3 were more sensitive to calcium depletion as seen by a more rapid drop in their cell index (Figure 3b).

To determine how reduced E-cadherin adhesion affects cellular functions, we cultivated cells in hanging drops, thus preventing cells from adhering to a substrate. Under these conditions, MCF7 cells aggregate, forming large spheroids. Visual inspection did not reveal any overt differences in the kinetics of cell aggregation, and after overnight incubation control and siDLC3 spheroids had a similar appearance. By pipetting spheroids up and down in a defined manner, cell adhesion strength can be examined. Cells lacking DLC3 were less resistant to trituration compared with control cells and disaggregated into small aggregates and single cells more readily (Figure 3c, see Supplementary Figure S3 for additional images). Loss of cell adhesion is often associated with increased motility. Indeed, directed migration assays through Transwell filters revealed that DLC3 downregulation increased cell motility (Figure 3d). Of note, in wounding assays no increased migration was observed (data not shown), which may be due to the fact that collective migration requires intact cell–cell adhesions. Together these data indicate that DLC3 is required for E-cadherin function and the maintenance of stable epithelial cell–cell adhesions.

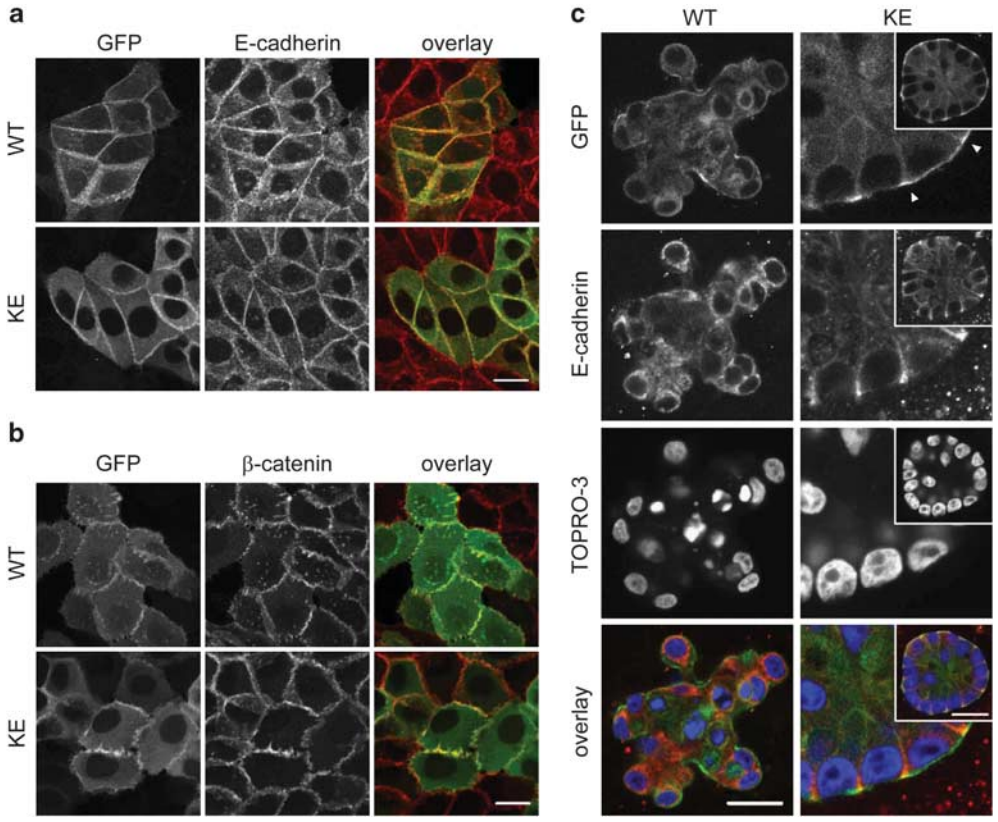

Figure 1. GFP–DLC3α co-localizes with E-cadherin at cell–cell adhesions and ectopic expression impairs differentiation of MCF10A cells in 3D cultures. (**a**) MCF7 and (**b**) MCF10A cells stably expressing wild-type and GAP-inactive (K725E) GFP-tagged DLC3α were stained with antibodies specific for E-cadherin and β-catenin (red), respectively. (**c**) MCF10A cells stably expressing wild-type and GAP-inactive (K725E) GFP–DLC3α were cultured in matrigel for 6 days and stained with an E-cadherin-specific antibody (red); nuclei were counterstained with TOPRO-3 (blue). (**a**) The images shown are stacks of several confocal sections and (**b**, **c**) single confocal sections. Scale bar, 20 μm.

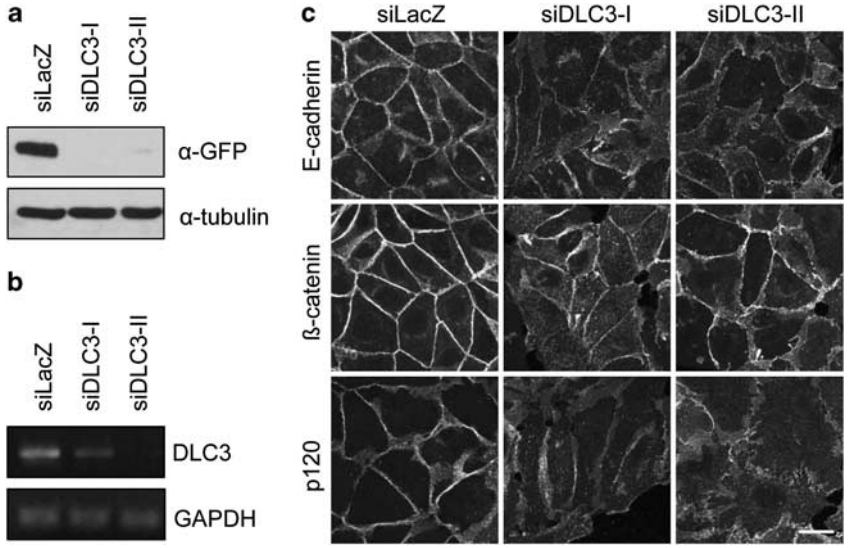

Figure 2. DLC3 depletion disrupts cell junctions. (**a**) HEK293T cells were transfected with a GFP–DLC3α expression plasmid along with siRNAs targeting DLC3 (siDLC3-I and siDLC3-II), respectively, or siLacZ. Cells were lysed 48 h post transfection and GFP–DLC3α expression was analyzed by immunoblotting with a GFP-specific antibody (top). The membrane was reprobed with a tubulin-specific antibody (bottom). (**b**) MCF7 cells were transfected with siLacZ, siDLC3-I and siDLC3-II, respectively. Post transfection (72 h), RNA was extracted and cDNA was analyzed by semi-quantitative RT–PCR using DLC3-specific primers. GADPH was amplified as a loading control. (**c**) MCF7 cells were transfected with siLacZ, siDLC3-I and siDLC3-II, respectively. Post transfection (72 h), cells were stained with antibodies specific for E-cadherin, β-catenin and p120-catenin. The images shown are stacks of several confocal sections. Scale bar, 20 μm.

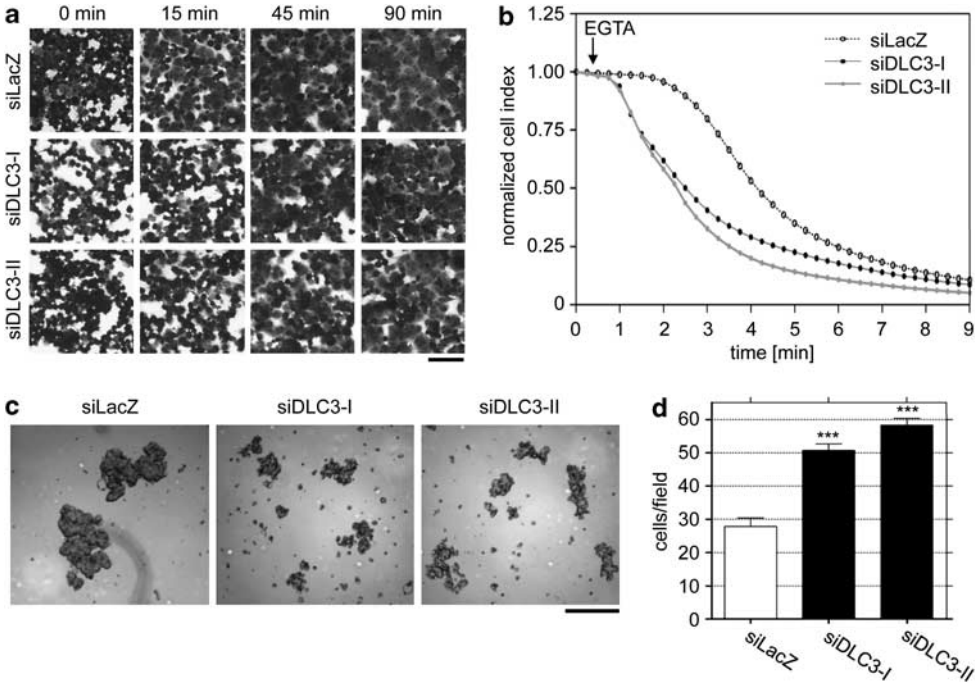

Figure 3. DLC3 depletion reduces cell–cell adhesion and increases cell motility. MCF7 cells were transfected with siLacZ, siDLC3-I and siDLC3-II, respectively. (**a**, **b**) Post transfection (48 h), cells were replated onto collagen-coated dishes. The next day, confluent cell monolayers were treated with 4 mM EGTA for 15 min. Cells were washed and incubated with fresh medium. In (**a**), cells were fixed and stained at the indicated times (scale bar, 100 μm), in (**b**) the normalized mean impedance (cell index) of duplicate wells measured with an xCELLigence device is plotted. (**c**) Post transfection (48 h), cells were suspended in hanging drops as described in the Materials ans methods section. The next day, spheroids were resuspended by pipetting and photographed. Scale bar, 200 μm. (**d**) Post transfection (72 h), cells in medium containing 0.5% FCS were plated into Transwell filters coated with collagen on the underside. The bottom chamber contained medium with 10% FCS. After overnight incubation, migrated cells were fixed and stained. Data shown are the mean ± s.e.m. of duplicate wells and are representative of 3 independent experiments. Values for siDLC3-I and siDLC3-II versus siLacZ were statistically significant (Student's *t*-test; ***$P < 0.001$).

DLC3 loss disrupts adherens junctions via aberrant Rho–ROCK signaling

Cell junctions are tightly associated with the actin cytoskeleton, the appearance of which depends on Rho activity. In the absence of DLC3 the perijunctional actin belt as visualized by phalloidin staining was severely disorganized (Figure 4a) and the cytoskeletal adapter protein vinculin, which localized to cell–cell adhesions in confluent control cells where it is known to contribute to stabilization of Ajs,[28] displayed increased redistribution to focal adhesions (Figure 4a). Constitutively active Rho has been reported to destabilize cell junctions through the ROCK signaling pathway.[14] To investigate the role of ROCK in DLC3-depleted cells, we treated cells overnight with the pharmacological ROCK inhibitor Y27632 before analysis by indirect immunofluorescence. ROCK inhibition had little effect on the appearance of β-catenin in siLacZ control cells. However, in DLC3-depleted cells ROCK inhibition restored junctional localization of β-catenin (Figure 4b). Similar results were obtained for E-cadherin (data not shown). Parallel staining of phosphorylated, active MLC not only revealed that ROCK inhibition was successful, but also showed that DLC3-depleted cells contained regions with elevated pMLC levels, indicative of aberrant local Rho–ROCK signaling (Figure 4b). Together our results identify DLC3 as a novel component of the E-cadherin regulatory network that is important for maintaining integrity of AJs through negative regulation of the Rho–ROCK signaling pathway.

DISCUSSION

Remodeling of adhesive cell–cell contacts occurs during epithelial morphogenesis, wound repair and cancer invasion, and is regulated by the coordinated activity of Rho GTPases. Disruption of RhoGAP88c, the DLC ortholog in Drosophila, led to abnormalities in various tissues undergoing morphogenetic movements and was associated with disorganized actin filament assembly. RhoGAP88C localizes basolaterally and is therefore thought to restrict Rho activity to the apical surface.[29,30] The potential contribution of the mammalian DLC proteins to epithelial morphogenesis has not been addressed. Here we show that ectopic expression of DLC3 in MCF10A breast epithelial cells interferes with normal acinar development in 3D cultures, most likely through inhibition of Rho signaling, because expression of a GAP-inactive DLC3 variant did not impair cell differentiation. In addition to GAP activity toward RhoA, DLC3 was reported to display modest activity for Cdc42 *in vitro*.[25] However, we did not detect any activity changes of a Cdc42 biosensor upon DLC3 overexpression, indicating that in intact cells DLC3 is specific for RhoA. Whether inactivation of RhoA alone is sufficient to induce the severe morphological changes observed remains to be investigated. It is possible that ectopic DLC3 expression also impacts RhoB and/or RhoC because RhoA knockdown in human mammary epithelial cells reduced apical orientation of the Golgi but basolateral distribution of E-cadherin and apicolateral distribution of F-actin were maintained.[31] Vice versa, constitutively active RhoA was shown to disrupt mammary epithelial cell morphogenesis through increased contractility due to aberrant ROCK activation.[32] However, stable downregulation of DLC3 in MCF10A cells did not have an obvious effect on cell differentiation in 3D cultures (data not shown), which may be due to redundant mechanisms that ensure acinus development.

The conserved structural composition of the three mammalian DLC proteins suggests overlapping cellular functions. *In vitro*, the DLC proteins all display substrate specificity toward RhoA and

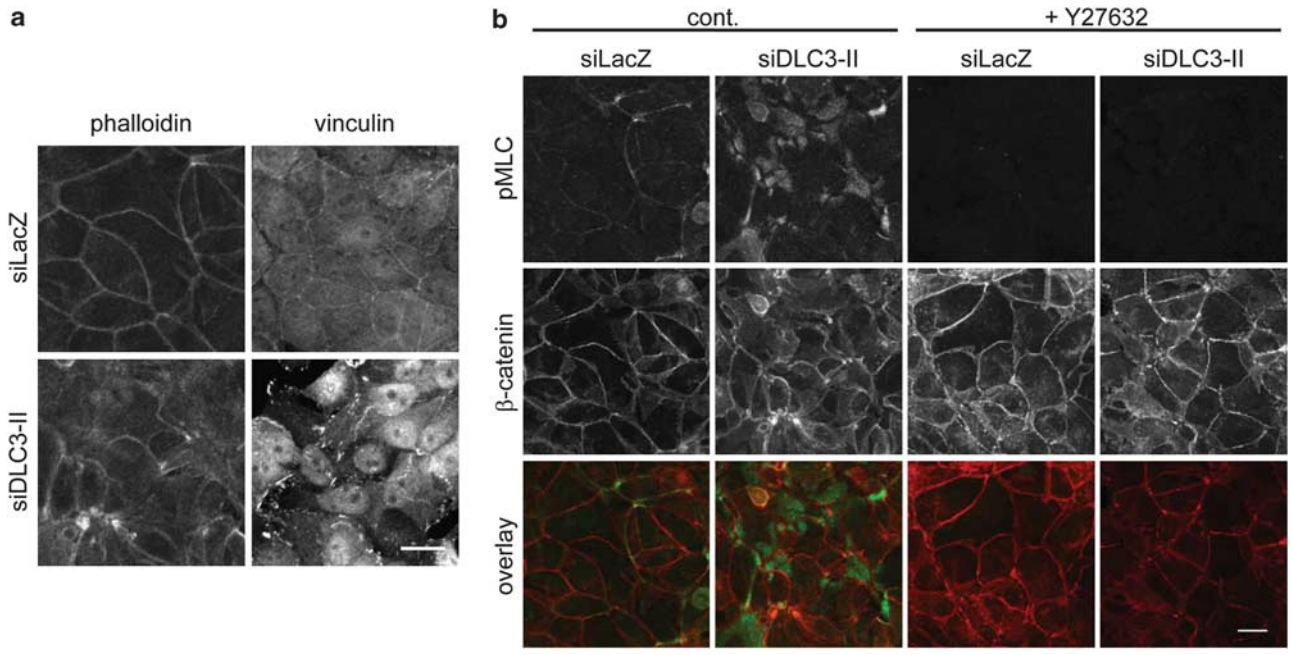

Figure 4. ROCK inhibition restores AJs in DLC3-depleted cells. (**a**, **b**) MCF7 cells were transfected with siLacZ and siDLC3-II. (**a**) Post transfection (72 h), cells were stained with a vinculin-specific antibody and AlexaFluor-546 conjugated phalloidin. (**b**) Two days post transfection, cells were treated overnight with 10 μM Y27632 or DMSO (cont.) before staining with antibodies specific for pMLC (green) and β-catenin (red). Images shown are stacks of several confocal sections. Scale bar, 20 μm.

their ectopic expression in cells has similar consequences, namely the dissolution of stress fibers and focal adhesions.[17,25] However, although DLC1 ablation in mice is embryonically lethal,[33,34] DLC2-deficient mice are viable and develop normally.[35,36] In MCF7 cells, which express all DLC isoforms, DLC1 knockdown stimulated directed cell migration through a Dia1-dependent pathway, whereas DLC2 knockdown failed to enhance cell motility.[37] We believe that these differences are due to the distinct subcellular localizations and regulation by different molecular mechanisms and protein partners. For example, in MCF7 cells, DLC1 but not DLC2 localizes to focal adhesions[37] and only DLC1 is regulated by PKD-mediated phosphorylation and 14-3-3 protein binding.[38] Interestingly, ectopic expression of DLC1 in MCF10A cells reduced acini size but did not interfere with cell polarization in 3D cultures, providing further support for isoform-specific functions (our unpublished observations).

In subconfluent MCF7 cells, GFP-tagged DLC3 was also found to localize to focal adhesions (data not shown), which is in agreement with a previous report on DLC3 localization in HeLa cells[25] and the interaction of DLC3α with tensin in coimmunoprecipations.[20] In confluent cell monolayers, DLC3 was redistributed to sites of cell–cell adhesion (Figure 1a, Supplementary Figure S1), whereas in 3D cultures it was enriched at the basolateral membrane especially at the edges of cell contacts (Figure 1c) where thick actin bundles, so-called actin arcs, are known to stabilize mature cell–cell adhesions.[1] Expression of the DLC3 wild-type protein may thus specifically interfere with the establishment of these stabilizing actin structures. It will be of particular interest to define the domains that target DLC3 to AJs and the molecular mechanisms that regulate its junctional recruitment and activation at these sites. As both DLC3α and DLC3β localized to cell–cell contacts, the SAM domain is not involved in junctional localization, nor is GAP activity required. Ectopic expression of E-cadherin in non-small cell lung cancer cell lines reduced RhoA activity, which was partially restored by downregulation of DLC1 or p190RhoGAP.[39] At the plasma membrane, p190RhoGAP associates with p120RasGAP[40] and p120RasGAP was identified to interact with DLC1 via the GAP domain in a yeast two hybrid screen.[41] Due to the high homology of the GAP domain across the DLC protein family, it is possible that DLC3 also complexes with p120RasGAP.

We recently reported that DLC1 GAP activity is stimulated by phosphatidylinositol 4,5-bisphosphate ($PI(4,5)P_2$) binding to a conserved polybasic region preceding the GAP domain.[42] This polybasic region is conserved in DLC3, raising the possibility that $PI(4,5)P_2$ contributes to DLC3 activation at AJs. $PI(4,5)P_2$ is generated by sequential phosphorylation of phosphatidylinositol by phosphatidylinositol 4-kinase and phosphatidylinositol-4-phosphate 5-kinase. Rac and Rho contribute to the recruitment to and activation of these lipid kinases at the plasma membrane[43] and phosphatidylinositol-4-phosphate 5-kinase has been shown to be activated during cell–cell adhesion to produce $PI(4,5)P_2$ at sites of cell–cell contact.[44] It is thus intriguing to speculate that Rho terminates its own activation by local generation of $PI(4,5)P_2$, which activates DLC3.

In summary, we conclude that DLC3 is required for the formation of stable AJs by spatially balancing Rho–ROCK signaling. Our data are in agreement with the observation that elevated Rho activity impairs E-cadherin function, as DLC3 knockdown increased calcium sensitivity of cells and impaired cell aggregation. ROCK inhibition resulted in a more punctate appearance of cell junctions, in line with reports on the requirement of ROCK and myosin II for E-cadherin accumulation at AJs.[45] Nevertheless, ROCK inhibition restored junctional localization of E-cadherin and β-catenin complexes and epithelial morphology in cells lacking DLC3 (see Figure 4b). Rho activation associated with carcinogenesis is mainly caused by deregulation of GEFs and GAPs. Of the more than 70 RhoGAP proteins, it is the DLC subfamily that is downregulated in many cancer types.[46] Impaired cell–cell adhesion, cytoplasmic distribution of catenins and enhanced motility are typical features of epithelial mesenchymal transition, a cellular program that is characterized by the loss of epithelial traits and the acquisition of a highly motile mesenchymal phenotype.[47] It is thus tempting to speculate that reduced DLC3 transcript levels

observed in different carcinomas[23] compromise epithelial integrity and facilitate epithelial-mesenchymal transition, thereby contributing to tumor progression.

MATERIALS AND METHODS

Antibodies and reagents

Antibodies used were: mouse anti-E-cadherin, anti-β-catenin, and anti-p120-catenin (BD, Heidelberg, Germany), rabbit anti-phospho-MLC and anti-E-cadherin pAbs (Cell Signaling, Danvers, MA, USA), rabbit anti-GFP pAb (Santa Cruz Biotechnology, Santa Cruz, CA, USA), and mouse anti-tubulin mAb (Sigma, St Louis, MO, USA). HRP-labeled secondary anti-mouse and anti-rabbit IgG antibodies were from GE Healthcare, Piscataway, NJ, USA; Alexa Fluor 488- and Alexa Fluor 546-labeled secondary anti-mouse and anti-rabbit IgG antibodies, and TOPRO3 were from Invitrogen, Karlsruhe, Germany. Y27632 was from Calbiochem, Darmstadt, Germany.

Cloning of DLC3 expression constructs

Cloning of expression vectors encoding DLC3α and DLC3β cDNAs have been described previously.[42] The DLC3β–K645E GAP-inactive mutant was generated by QuikChange site-directed PCR mutagenesis (Stratagene, La Jolla, CA, USA) using pEGFPC1–DLC3β as a template. The forward primer used was: DLC3-K645E-for (5′-GTGGCTGACCTGCTAGAGCAGTATTTCCGGGAC-3′). To generate pEGFPC1–DLC3α–K725E, pEGFPC1–DLC3α was digested with *Hin*dIII and *Bpi*I and the fragment corresponding to the DLC3α 5′ region was ligated with pEGFPC1–DLC3β–K645E digested with *Hin*dIII and *Bpi*I. All amplified cDNAs were verified by sequencing. Full-length DLC3α and DLC3β were subcloned from the pEGFP–C1 vectors by *Eco*RI restriction into the pmCherry-C1 vector. Retroviral expression vectors were generated by digestion of pEGFPC1–DLC3α and pEGFPC1–DLC3α-K725E with *Nhe*I, followed by fill-in with Klenow polymerase and digestion with *Sal*I. These expression cassettes were ligated with the pBABE-Puro vector digested with *Sna*BI and *Sal*I. Oligonucleotides were purchased from MWG Biotech, Ebersberg, Germany.

Cell culture, transfection and generation of stable cell lines

MCF7 and HEK293T cells were cultured in RPMI 1640 (Invitrogen), and Plat-E cells in DMEM medium (Invitrogen) supplemented with 10% FCS (PAA) and incubated in a humidified atmosphere of 5% CO_2 at 37 °C. MCF10A cells stably expressing the ecotropic receptor (MCF10A-ecoR[27]), a kind gift of Drs Danielle Carroll and Joan Brugge, were cultivated in DMEM/F12 medium (Invitrogen) supplemented with 5% horse serum (Invitrogen), 20 ng/ml EGF (R&D), 10 μg/ml insulin (Sigma), 0.5 μg/ml hydrocortisone (Sigma), 100 ng/ml cholera toxin (Sigma), 50 U/ml penicillin and 50 mg/ml streptomycin (Invitrogen). HEK293T and Plat-E cells were transfected with TransIT (Mirus) according to manufacturer's instructions. Stable MCF7 sublines cells were generated by nucleofection (program X005, Kit V) with pEGFPC1–DLC3 expression vectors followed by selection with 1 mg/ml G418 (Calbiochem). Stable MCF10A sublines were generated by retroviral transduction using supernatants from Plat-E cells transfected with pBABE-Puro DLC3 expression vectors. Supernatants were harvested after 48 h and filtered (0.45 μm). The supernatants were mixed at a 1:1 ratio with MCF10A growth medium, polybrene (Sigma) was added to a final concentration of 8 μg/ml and added to the cells. After 48 h, cells were selected with 1.5 μg/ml puromycin (Sigma) for two weeks, followed by FACS sorting of GFP-positive cells. Stable expression of the GFP-tagged DLC3 proteins in the MCF7 and MCF10A sublines was verified by FACS analysis and immunoblotting. For MCF10A 3D cultures, 4-well culture slides (BD) were coated with 80 μl matrigel (BD) and left to solidy at 37 °C for 15 min. In total, 4000 cells in 800 μl assay medium (DMEM/F12 with 2% horse serum, 10 μg/ml insulin, 0.5 μg/ml hydrocortisone, 100 ng/ml cholera toxin, 5 ng/ml EGF, 50 U/ml penicillin and 50 mg/ml streptomycin) supplemented with 2% matrigel were seeded in each chamber and cells were refed twice a week. For RNA interference, cells were transfected with siRNA using Oligofectamine (Invitrogen) according to manufacturer's instructions. The siRNAs used were: 5′-UAGCCACAGUUGAGGUCAAdTdT-3′ (siDLC3-I), 5′-UCUCUGAGGCGGAAGGAAAdTdT-3′ (siDLC3-II), and 5′-GCGGCUGCCGGAAUUUACCdTdT-3′ (siLacZ). All siRNAs were obtained from MWG Biotech.

Semi-quantitative RT–PCR

RNA was extracted using a PureLink Total RNA purification kit (Invitrogen) and reverse transcribed using the First Strand cDNA Synthesis Kit with random hexamer primers (Fermentas, St Leon-Rot, Germany). The cDNA was then used as a template for PCR analysis with REDTaq PCR Master Mix (Sigma). Primers used were: DLC3-F (5′-CTGGACCAAGTAGGCATCTTCC-3′) and DLC3-R (5′-CTCTTCCATGTAGAGGCTCAGG-3′); GAPDH-F (5′-CCCCTTCATTGACCTCAACTA-3′) and GAPDH-R (5′-CGCTCCTGGAAGATGGTGAT-3′).

Cell lysis, SDS–PAGE and western blotting

Cells were lysed in RIPA buffer (50 mM Tris (pH 7.5), 150 mM NaCl, 1% NP-40, 0.5% sodium deoxycholate, 0.1% SDS, 1 mM sodium orthovanadate, 10 mM sodium fluoride and 20 mM β-glycerophosphate plus Complete protease inhibitors (Roche)) and lysates were clarified by centrifugation at 16 000 *g* for 10 min. Equal amounts of protein were separated by SDS–PAGE and transferred to PVDF membrane (Roth). Membranes were blocked with 0.5% blocking reagent (Roche) in PBS containing 0.1% Tween-20 and incubated with primary antibodies, followed by HRP-conjugated secondary antibodies. Visualization was with the ECL detection system (Pierce, Rockford, IL, USA).

Immunofluorescence microscopy

Cells grown on glass coverslips coated with 25 μg/ml collagen (Serva) were fixed with 4% PFA for 10 min, permeabilized with PBS containing 0.1% Triton X-100 for 5 min and blocked with 5% goat serum (Invitrogen) in PBS containing 0.1% Tween-20. Cells were then incubated with primary antibodies in blocking buffer, washed with PBS containing 0.1% Tween-20 and incubated with secondary antibody in blocking buffer. MCF10A 3D cultures were fixed in 2% PFA for 20 min and permeabilized with 0.5% Triton X-100 in PBS for 15 min at 4 °C. After blocking with 10% goat serum and 0.2% Triton X-100 in PBS, cells were immunostained with primary antibodies diluted in blocking buffer overnight at 4 °C. Samples were washed with 0.2% Triton X-100 in PBS and incubated with secondary antibodies in blocking buffer at RT. Nuclei were counterstained with TOPRO-3 and slides were mounted in Fluoromount-G. All samples were analyzed on a confocal laser scanning microscope (Zeiss LSM 700) using 488, 561 and 633 nm excitation with the oil objective lenses EC Plan-Neofluar 40 × /1.30 DIC M27 and Plan-Apochromat 63 × /1.40 DIC M27. Images were processed with the ZEN software.

Calcium switch assays

Cells were harvested 2 days post transfection and replated at high density into 6-well dishes and 96-well E-plates (Roche, Mannheim, Germany), respectively. The next day, confluent cell monolayers were washed with HBSS (Invitrogen) and treated with 4 mM EGTA in HBSS for 10–15 min at 37 °C. Cells were again washed with HBSS, incubated with fresh medium for the indicated times, then fixed with 2% PFA containing 0.05% crystal violet and photographed (Leitz DM IRB). For quantitative analyses, the impedance of cells seeded into 96-well E-plates was measured using an xCELLigence device (Roche).

Cell disaggregation and migration assays

Cells were resuspended at a concentration of 1×10^6 cells/ml. 35 μl drops were pipetted into the lid of a cell culture dish and turned upside down. Cells were allowed to aggregate overnight and aggregates were photographed at a 10-fold magnification after pipetting up and down (15 × with a 20 μl pipette) (Leitz DM IRB). Cell migration assays were performed as described previously.[37]

Rho GTPase biosensor assays

Biosensor assays were performed as described previously.[37] In brief, HEK293T cells were transfected with either Raichu-RhoA, -Rac1 or -Cdc42 biosensor plasmids together with empty vector or expression vectors encoding different mCherry-DLC3 variants. The next day, cell lysates were prepared and emission ratios (FRET/CFP) were determined by measuring CFP and YFP fluorescence after background subtraction at 475 and 530 nm, respectively, using a Tecan Infinite 200M plate reader (excitation, 433 nm). Expression levels of the biosensor were monitored by measuring YFP fluorescence (excitation, 480 nm) and those of the DLC3 variants by measuring mCherry fluorescence (excitation, 575 nm and emission, 615 nm).

CONFLICT OF INTEREST

The authors declare no conflict of interest.

ACKNOWLEDGEMENTS

We wish to thank Cornelius Knabbe, Angelika Hausser, Danielle Carroll and Joan Brugge for MCF7, HEK293T, and MCF10A-ecoR cells, respectively, and Michiyuki Matsuda for the Raichu biosensors. TB is supported by the DFG Emmy-Noether-Program and the CRC 850. This work was supported by DFG 587259 and DKH 109033 grants to MAO.

REFERENCES

1 Cavey M, Lecuit T. Molecular bases of cell-cell junctions stability and dynamics. *Cold Spring Harb Perspect Biol* 2009; **1**: a002998.
2 Harris TJ, Tepass U. Adherens junctions: from molecules to morphogenesis. *Nat Rev Mol Cell Biol* 2010; **11**: 502–514.
3 Iden S, Collard JG. Crosstalk between small GTPases and polarity proteins in cell polarization. *Nat Rev Mol Cell Biol* 2008; **9**: 846–859.
4 Samarin S, Nusrat A. Regulation of epithelial apical junctional complex by Rho family GTPases. *Front Biosci* 2009; **14**: 1129–1142.
5 Yamada S, Nelson WJ. Localized zones of Rho and Rac activities drive initiation and expansion of epithelial cell-cell adhesion. *J Cell Biol* 2007; **178**: 517–527.
6 Sahai E, Marshall CJ. ROCK and Dia have opposing effects on adherens junctions downstream of Rho. *Nat Cell Biol* 2002; **4**: 408–415.
7 Riento K, Ridley AJ. Rocks: multifunctional kinases in cell behaviour. *Nat Rev Mol Cell Biol* 2003; **4**: 446–456.
8 Carramusa L, Ballestrem C, Zilberman Y, Bershadsky AD. Mammalian diaphanous-related formin Dia1 controls the organization of E-cadherin-mediated cell-cell junctions. *J Cell Sci* 2007; **120**: 3870–3882.
9 Wallace SW, Magalhaes A, Hall A. The Rho target PRK2 regulates apical junction formation in human bronchial epithelial cells. *Mol Cell Biol* 2011; **31**: 81–91.
10 Calautti E, Grossi M, Mammucari C, Aoyama Y, Pirro M, Ono Y *et al.* Fyn tyrosine kinase is a downstream mediator of Rho/PRK2 function in keratinocyte cell-cell adhesion. *J Cell Biol* 2002; **156**: 137–148.
11 Bos JL, Rehmann H, Wittinghofer A. GEFs and GAPs: critical elements in the control of small G proteins. *Cell* 2007; **129**: 865–877.
12 Terry SJ, Zihni C, Elbediwy A, Vitiello E, Leefa IV CS, Balda MS *et al.* Spatially restricted activation of RhoA signalling at epithelial junctions by p114RhoGEF drives junction formation and morphogenesis. *Nat Cell Biol* 2011; **13**: 159–166.
13 Samarin SN, Ivanov AI, Flatau G, Parkos CA, Nusrat A. Rho/Rho-associated kinase-II signaling mediates disassembly of epithelial apical junctions. *Mol Biol Cell* 2007; **18**: 3429–3439.
14 Wildenberg GA, Dohn MR, Carnahan RH, Davis MA, Lobdell NA, Settleman J *et al.* p120-catenin and p190RhoGAP regulate cell-cell adhesion by coordinating antagonism between Rac and Rho. *Cell* 2006; **127**: 1027–1039.
15 Nimnual AS, Taylor LJ, Bar-Sagi D. Redox-dependent downregulation of Rho by Rac. *Nat Cell Biol* 2003; **5**: 236–241.
16 Sander EE, ten Klooster JP, van Delft S, van der Kammen RA, Collard JG. Rac downregulates Rho activity: reciprocal balance between both GTPases determines cellular morphology and migratory behavior. *J Cell Biol* 1999; **147**: 1009–1022.
17 Durkin ME, Yuan BZ, Zhou X, Zimonjic DB, Lowy DR, Thorgeirsson SS *et al.* DLC-1:a Rho GTPase-activating protein and tumour suppressor. *J Cell Mol Med* 2007; **11**: 1185–1207.
18 Xue W, Krasnitz A, Lucito R, Sordella R, Vanaelst L, Cordon-Cardo C *et al.* DLC1 is a chromosome 8p tumor suppressor whose loss promotes hepatocellular carcinoma. *Genes Dev* 2008; **22**: 1439–1444.
19 Goodison S, Yuan J, Sloan D, Kim R, Li C, Popescu NC *et al.* The RhoGAP protein DLC-1 functions as a metastasis suppressor in breast cancer cells. *Cancer Res* 2005; **65**: 6042–6053.
20 Qian X, Li G, Asmussen HK, Asnaghi L, Vass WC, Braverman R *et al.* Oncogenic inhibition by a deleted in liver cancer gene requires cooperation between tensin binding and Rho-specific GTPase-activating protein activities. *Proc Natl Acad Sci USA* 2007; **104**: 9012–9017.
21 Yam JW, Ko FC, Chan CY, Jin DY, Ng IO. Interaction of deleted in liver cancer 1 with tensin2 in caveolae and implications in tumor suppression. *Cancer Res* 2006; **66**: 8367–8372.
22 Liao YC, Si L, deVere White RW, Lo SH. The phosphotyrosine-independent interaction of DLC-1 and the SH2 domain of cten regulates focal adhesion localization and growth suppression activity of DLC-1. *J Cell Biol* 2007; **176**: 43–49.
23 Durkin ME, Ullmannova V, Guan M, Popescu NC. Deleted in liver cancer 3 (DLC-3), a novel Rho GTPase-activating protein, is downregulated in cancer and inhibits tumor cell growth. *Oncogene* 2007; **26**: 4580–4589.
24 Yoshizaki H, Ohba Y, Kurokawa K, Itoh RE, Nakamura T, Mochizuki N *et al.* Activity of Rho-family GTPases during cell division as visualized with FRET-based probes. *J Cell Biol* 2003; **162**: 223–232.
25 Kawai K, Kiyota M, Seike J, Deki Y, Yagisawa H. START-GAP 3/DLC3 is a GAP for RhoA and Cdc42 and is localized in focal adhesions regulating cell morphology. *Biochem Biophys Res Commun* 2007; **364**: 783–789.
26 Debnath J, Brugge JS. Modelling glandular epithelial cancers in three-dimensional cultures. *Nat Rev Cancer* 2005; **5**: 675–688.
27 Brummer T, Schramek D, Hayes VM, Bennett HL, Caldon CE, Musgrove EA *et al.* Increased proliferation and altered growth factor dependence of human mammary epithelial cells overexpressing the Gab2 docking protein. *J Biol Chem* 2006; **281**: 626–637.
28 Carisey A, Ballestrem C. Vinculin an adapter protein in control of cell adhesion signalling. *Eur J Cell Biol* 2011; **90**: 157–163.
29 Denholm B, Brown S, Ray RP, Ruiz-Gomez M, Skaer H, Hombria JC. Crossveinless-c is a RhoGAP required for actin reorganisation during morphogenesis. *Development* 2005; **132**: 2389–2400.
30 Brodu V, Casanova J. The RhoGAP crossveinless-c links trachealess and EGFR signaling to cell shape remodeling in Drosophila tracheal invagination. *Genes Dev* 2006; **20**: 1817–1828.
31 Duan L, Chen G, Virmani S, Ying G, Raja SM, Chung BM *et al.* Distinct roles for Rho versus Rac/Cdc42 GTPases downstream of Vav2 in regulating mammary epithelial acinar architecture. *J Biol Chem* 2010; **285**: 1555–1568.
32 Paszek MJ, Zahir N, Johnson KR, Lakins JN, Rozenberg GI, Gefen A *et al.* Tensional homeostasis and the malignant phenotype. *Cancer Cell* 2005; **8**: 241–254.
33 Durkin ME, Avner MR, Huh CG, Yuan BZ, Thorgeirsson SS, Popescu NC. DLC-1 a Rho GTPase-activating protein with tumor suppressor function, is essential for embryonic development. *FEBS Lett* 2005; **579**: 1191–1196.
34 Sabbir MG, Wigle N, Loewen S, Gu Y, Buse C, Hicks GG *et al.* Identification and characterization of Dlc1 isoforms in the mouse and study of the biological function of a single gene trapped isoform. *BMC Biol* 2010; **8**: 17.
35 Yau TO, Leung TH, Lam S, Cheung OF, Tung EK, Khong PL *et al.* Deleted in liver cancer 2 (DLC2) was dispensable for development and its deficiency did not aggravate hepatocarcinogenesis. *PLoS One* 2009; **4**: e6566.
36 Lin Y, Chen NT, Shih YP, Liao YC, Xue L, Lo SH. DLC2 modulates angiogenic responses in vascular endothelial cells by regulating cell attachment and migration. *Oncogene* 2010; **29**: 3010–3016.
37 Holeiter G, Heering J, Erlmann P, Schmid S, Jahne R, Olayioye MA. Deleted in liver cancer 1 controls cell migration through a Dia1-dependent signaling pathway. *Cancer Res* 2008; **68**: 8743–8751.
38 Scholz RP, Regner J, Theil A, Erlmann P, Holeiter G, Jahne R *et al.* DLC1 interacts with 14-3-3 proteins to inhibit RhoGAP activity and block nucleocytoplasmic shuttling. *J Cell Sci* 2009; **122**: 92–102.
39 Asnaghi L, Vass WC, Quadri R, Day PM, Qian X, Braverman R *et al.* E-cadherin negatively regulates neoplastic growth in non-small cell lung cancer: role of Rho GTPases. *Oncogene* 2010; **29**: 2760–2771.
40 Kulkarni SV, Gish G, van der GP, Henkemeyer M, Pawson T. Role of p120 Ras-GAP in directed cell movement. *J Cell Biol* 2000; **149**: 457–470.
41 Yang XY, Guan M, Vigil D, Der CJ, Lowy DR, Popescu NC. p120Ras-GAP binds the DLC1 Rho-GAP tumor suppressor protein and inhibits its RhoA GTPase and growth-suppressing activities. *Oncogene* 2009; **28**: 1401–1409.
42 Erlmann P, Schmid S, Horenkamp FA, Geyer M, Pomorski TG, Olayioye MA. DLC1 activation requires lipid interaction through a polybasic region preceding the RhoGAP domain. *Mol Biol Cell* 2009; **20**: 4400–4411.
43 Santarius M, Lee CH, Anderson RA. Supervised membrane swimming: small G-protein lifeguards regulate PIPK signalling and monitor intracellular PtdIns(4,5)P2 pools. *Biochem J* 2006; **398**: 1–13.
44 El Sayegh TY, Arora PD, Ling K, Laschinger C, Janmey PA, Anderson RA *et al.* Phosphatidylinositol-4,5 bisphosphate produced by PIP5KIgamma regulates gelsolin, actin assembly, and adhesion strength of N-cadherin junctions. *Mol Biol Cell* 2007; **18**: 3026–3038.
45 Shewan AM, Maddugoda M, Kraemer A, Stehbens SJ, Verma S, Kovacs EM *et al.* Myosin 2 is a key Rho kinase target necessary for the local concentration of E-cadherin at cell-cell contacts. *Mol Biol Cell* 2005; **16**: 4531–4542.
46 Vigil D, Cherfils J, Rossman KL, Der CJ. Ras superfamily GEFs and GAPs: validated and tractable targets for cancer therapy? *Nat Rev Cancer* 2010; **10**: 842–857.
47 Yilmaz M, EMT Christofori G. the cytoskeleton, and cancer cell invasion. *Cancer Metastasis Rev* 2009; **28**: 15–33.

Supplementary Information accompanies the paper on the Oncogenesis website (http://www.nature.com/oncsis)